Remote Sensing of Environment 131 (2013) 215–231

Contents lists available at SciVerse ScienceDirect

Remote Sensing of Environment

journal homepage: www.elsevier.com/locate/rse

MODIS-based corn grain yield estimation model incorporating crop phenology information

Toshihiro Sakamoto [a,*], Anatoly A. Gitelson [b], Timothy J. Arkebauer [c]

[a] Ecosystem Informatics Division, National Institute for Agro-Environmental Sciences, Tsukuba, Ibaraki, Japan
[b] Center for Advanced Land Management Information Technologies, School of Natural Resources, University of Nebraska-Lincoln, Lincoln, NE, USA
[c] Department of Agronomy and Horticulture, University of Nebraska-Lincoln, Lincoln, NE, USA

ARTICLE INFO

Article history:
Received 7 October 2012
Received in revised form 13 December 2012
Accepted 14 December 2012
Available online xxxx

Keywords:
Crop phenology
Green LAI
MODIS
Shape-model fitting
U.S. Corn Belt

ABSTRACT

A crop yield estimation model using time-series MODIS WDRVI was developed. The main feature of the proposed model is the incorporation of crop phenology detection using MODIS data, called the "Shape-Model Fitting Method". MODIS WDRVI taken 7–10 days before the corn silking stage had strong linear correlation with corn final grain yield at both field and regional scales. The model revealed spatial patterns of corn final grain yield all over the U.S. from 2000 to 2011. State-level corn yield was estimated accurately with coefficient of variation below 10% especially for the 18 major corn producing states including Iowa, Illinois, Delaware, Minnesota, Ohio, West Virginia, Wisconsin, Michigan, Indiana, Nebraska, Kentucky, New York, South Dakota, Missouri, Pennsylvania, Tennessee, New Jersey and Maryland. The results corresponded well with the spatial pattern of high-yield regions derived from the USDA/NASS data. However, the model tended to underestimate corn grain yield in three irrigated regions: the Midwestern region depending on the Ogallala Aquifer, the downstream basin of the Mississippi, and the southwestern region of Georgia. In contrast, it tended to overestimate corn grain yield around the outlying regions of the U.S. Corn Belt, specifically, the East Coast, North Dakota, Minnesota, Wisconsin, and Missouri. The estimation accuracy of the proposed model differed depending on the region. However, the annual variation of state level corn grain yield could be detected with high accuracy, especially in the major corn producing states.

1. Introduction

The United States (U.S.) is the world's largest grain exporter. The total amount of corn exported in 2010/2011 was 45 million tons, which accounted for 49.2% of the world corn trade for that period (USDA/FAS, 2012). Thus, estimating grain yield over large areas as early as possible in the season is essential for not only the U.S. corn producers but also decision makers of food importing countries.

Various techniques based on remotely sensed data have been employed for assessment of crop yield (Bauer, 1975; Nellis et al., 2009). Idso et al. (1977) used infrared thermometers to observe leaf temperature during the reproductive stage and then developed the "stress degree day (SDD)" concept for predicting wheat grain yield. Since remote sensing based crop phenology detection was an integral part of the SDD approach, it was suggested that the seasonal profile of albedo (Idso et al., 1977) and the Simple Ratio (Hatfield, 1983) could be used for defining the reproductive stage. A wide variety of remote sensing based indicators were used in a simple regression between vegetation indices (VIs) and yield. Kogan (1997) developed the Vegetation Condition Index (VCI) and Temperature Condition Index (TCI) for global drought observation using NOAA/AVHRR. Both indices were found to have a high correlation with yield of corn (Unganai & Kogan, 1998), soybean (Liu & Kogan, 2002), winter wheat (Salazar et al., 2007), and cotton (Domenikiotis et al., 2004). Tennakoon et al. (1992) found a close correlation between four reflectance values of Landsat/TM bands (blue: 0.45–0.52 μm, red: 0.63–0.69 μm, and shortwave infrared: 1.55–1.75 μm and 2.08–2.35 μm) at the maturity stage of rice crop and the actual rice yield in Thailand. Serrano et al. (2000) found a good linear correlation between the cumulative total value of the Simple Ratio, taken from close range observations, and winter wheat yield. Labus et al. (2002) showed a strong relationship between wheat yield and integrated NDVI over the entire growing season on a regional and farm level in Montana, U.S. Ferencz et al. (2004) developed a General Yield Unified Reference Index (GYURI), which was the cumulative total value of the greenness (GN: NIR–red) filtered by double Gaussian curves, for crop yield estimation using NOAA–AVHRR, and showed a close correlation of GYURI with yields of eight different crops (corn, wheat, sugar beet, barley, alfalfa, rye, maize for silage, and pea) in Hungary. In addition, remote sensing derived VIs were often incorporated with meteorological data and a crop growth simulation model to obtain a synergistic effect on yield estimation accuracy (Boken & Shaykewich, 2002; Bouman, 1995; Doraiswamy et al., 2005; Maas, 1988; Moriondo et al., 2007; Rudorff & Batista, 1991).

* Corresponding author. Tel.: +81 29 838 8228.
E-mail address: sakamt@affrc.go.jp (T. Sakamoto).

0034-4257/$ – see front matter © 2013 Elsevier Inc. All rights reserved.
http://dx.doi.org/10.1016/j.rse.2012.12.017

While the final actual yield is considered to be determined by environmental stress during the reproductive stage (Idso et al., 1979a, 1979b), the potential amount of photosynthesis during the reproductive stage is dependent on the green LAI resulting from crop growth during the vegetative stage, which peaks around the tasseling stage for corn (Sakamoto et al., 2012). As examples of previous research of the relationship between VIs and final grain yield, Chang et al. (2005) found a close linear correlation between two ratio indices (NIR/red and NIR/green) at the booting stage of rice crop and the final rice grain yield. Ren et al. (2008) obtained a similar result, showing that the spatial accumulation of MODIS-NDVI at the booting–heading stage of winter wheat had the highest correlation with regional winter wheat production.

With respect to corn grain yield estimation, Guindin-Garcia (2010) found that green LAI during the mid-grain filling period (from milk [R3] to dough [R4] stage) is the best predictor of corn final grain yield and then showed that the MODIS Wide Dynamic Range Vegetation Index (WDRVI; Gitelson, 2004), taken during the mid-grain filling period in Nebraska, Iowa, and Illinois, was able to estimate county-level corn grain yield with high accuracy. Guindin-Garcia (2010) determined the phenological dates with statistical data published in a USDA Crop Progress Report (CPR), which was aggregated by a sub-state level administrative boundary called the Agricultural Statistics District (ASD). Although it is necessary to have a clear understanding of the spatial heterogeneity of the crop developmental stage for regional scale crop yield estimation, most states disclosed only state level data related to the crop developmental stage, with the exception of Illinois, Iowa, Kansas, and Missouri. Moreover, there are no available data for crop phenology in New York, New Jersey, Georgia, and Florida. Therefore, it is difficult to apply Guindin-Garcia's (2010) approach all over the U.S. when considering the existence of spatial variation of crop phenology within a state.

A temporal profile technology using multi-date Landsat MSS greenness data, which is a curve fitting approach, was proposed to estimate developmental stages of corn (Badhwar & Henderson, 1981) and soybeans (Henderson & Badhwar, 1984). In addition, it was applied to classify crop types (e.g., corn, soybean and others) in reference to parametric characteristics related to morphological and phenological differences (Badhwar et al., 1982; Hall & Badhwar, 1987). A crop phenology detection method using time series MODIS data has been developed recently (Sakamoto et al., 2010); it moved a step closer to practical use of remote sensing for crop yield estimation. Against this background, this study aimed to 1) improve Guindin-Garcia's (2010) approach by incorporating the crop phenology detection method and 2) explore the potential of MODIS time series data to estimate the spatial distribution of corn grain yield all over the U.S. for more than a decade.

2. Study area

Model calibration and validation were conducted on two different scales. One was a field-scale investigation using field experimental data. The other was a regional-scale investigation using county or state level agricultural statistics. For the field-scale investigation, three experimental sites located at the University of Nebraska-Lincoln (UNL) Agricultural Research and Development Center near Mead, Nebraska, U.S. (black star on Fig. 1a) were selected. Corn biophysical parameters and final grain yield have been surveyed there since 2001 as part of the UNL Carbon Sequestration Program (CSP). While sites 1 and 2 were irrigated by a center pivot irrigation system, site 3 was cultivated under a rainfed condition (Fig. 2). Site 1 has been continuously planted in corn since 2001. Sites 2 and 3 have been planted in a corn (odd years) and soybean (even years) rotation, though corn was grown at site 2 in 2010 as an exceptional case.

For the regional-scale investigation, the 35 states shown in Fig. 1a were selected for application of MODIS-based corn yield estimation model to reveal the spatio-temporal pattern of U.S. corn grain yield. Fig. 1b shows the spatial distribution of corn-cropping intensity on a county level in 2009. The data were downloaded from a web-accessible database called "QuickStats 2.0" provided by USDA/NASS.

3. Materials

3.1. MODIS WDRVI

This study used an 8-day time series of 250 m and 500 m MODIS surface reflectance data obtained by Terra (EOS AM) and Aqua (EOS PM). The MODIS products are distributed through NASA's Earth Observing System Data and Information System (EOSDIS). The MODIS datasets downloaded from EOSDIS were MOD09Q1, MOD09A1, MYD09Q1, and MYD09A1 (Collection 5, tile: h08v04, h08v05, h09v04, h08v05, h09v06, h10v04, h10v05, h10v06, h11v04, h11v05, h12v04, h12v05, and h13v04). The spatial resolutions of the MODIS 250-m (MOD09Q1, MYD09Q1) and 500-m products (MOD09A1, MYD09A1) were 231.7 m and 463.3 m, respectively. The map projection is sinusoidal projection. The red parallelograms in Fig. 2 show the footprints of MODIS 250 m pixels (sinusoidal projection) over a Landsat5 TM false color image projected by Universal Transverse Mercator (UTM). The MODIS 8-day composite products were systematically corrected for the effects of gaseous and aerosol scattering (Vermote & Vermeulen, 1999), providing the best surface spectral reflectance data for each 8-day period using the constrained view-angle maximum value composite method (Huete et al., 2002). Even with the systematic atmospheric correction, the spectral response of the target MODIS pixel is susceptible to the mixed-pixel effect due to surrounding land cover types. This is because with increasing sensor view angle the actual footprint of each MODIS pixel is larger than that of the nadir view footprint.

Numerical computation using the time series MODIS images was conducted on a pixel to pixel basis under the original sinusoidal map projection, and then the calculated results, such as corn silking date and corn grain yield, were compiled according to administrative boundary in dBase's underlying file format (dbf). Finally, the results were visualized by linking the dbf with a polygon data file (shape file) based on the Federal Information Processing Standard (FIPS) codes of each administrative territory under geographic projection.

The data layers of 250 m red (Band 1) and near infrared (NIR) reflectance (Band 2), which were included in the MOD09Q1 and MYD09Q1 products, were used in WDRVI calculations. The data layers of 500 m blue (Band 3) reflectance and observation date (day of year, DOY), which were included in the MOD09A1 and MYD09A1 products, were resampled from 500 m to 250 m resolution using the nearest neighbor method. Then they were used as criteria for cloud-cover pixel and observational date of each composite pixel for time-series processing called "Shape model fitting".

The WDRVI (Gitelson, 2004; Gitelson et al., 2007) was devised to linearize the relationship between green LAI and VI, based on red and NIR reflectance, using a weighting coefficient (α) in the following equation:

$$\mathrm{WDRVI} = (\alpha \times \rho_{\mathrm{NIR}} - \rho_{\mathrm{red}})/(\alpha \times \rho_{\mathrm{NIR}} + \rho_{\mathrm{red}}) \quad (1)$$

where ρ_{red} and ρ_{NIR} are the MODIS surface reflectances in the red (621–670 nm) and NIR (841–875 nm) bands, respectively. According to Guindin-Garcia et al. (2012), WDRVI with $\alpha = 0.1$ showed strong linear correlation with corn green LAI. We, therefore, assigned 0.1 to α for WDRVI and referred to this proxy of corn green LAI as WDRVI ($\alpha = 0.1$) in this study.

3.2. NASS-Cropland Data Layer

This study used the NASS Cropland Data Layer (NASS-CDL) for selection of target corn pixels. The coverage area of NASS-CDL was expanded from 6 states in 2000 to 40 states in 2009 (Fig. 14 a0–a11).

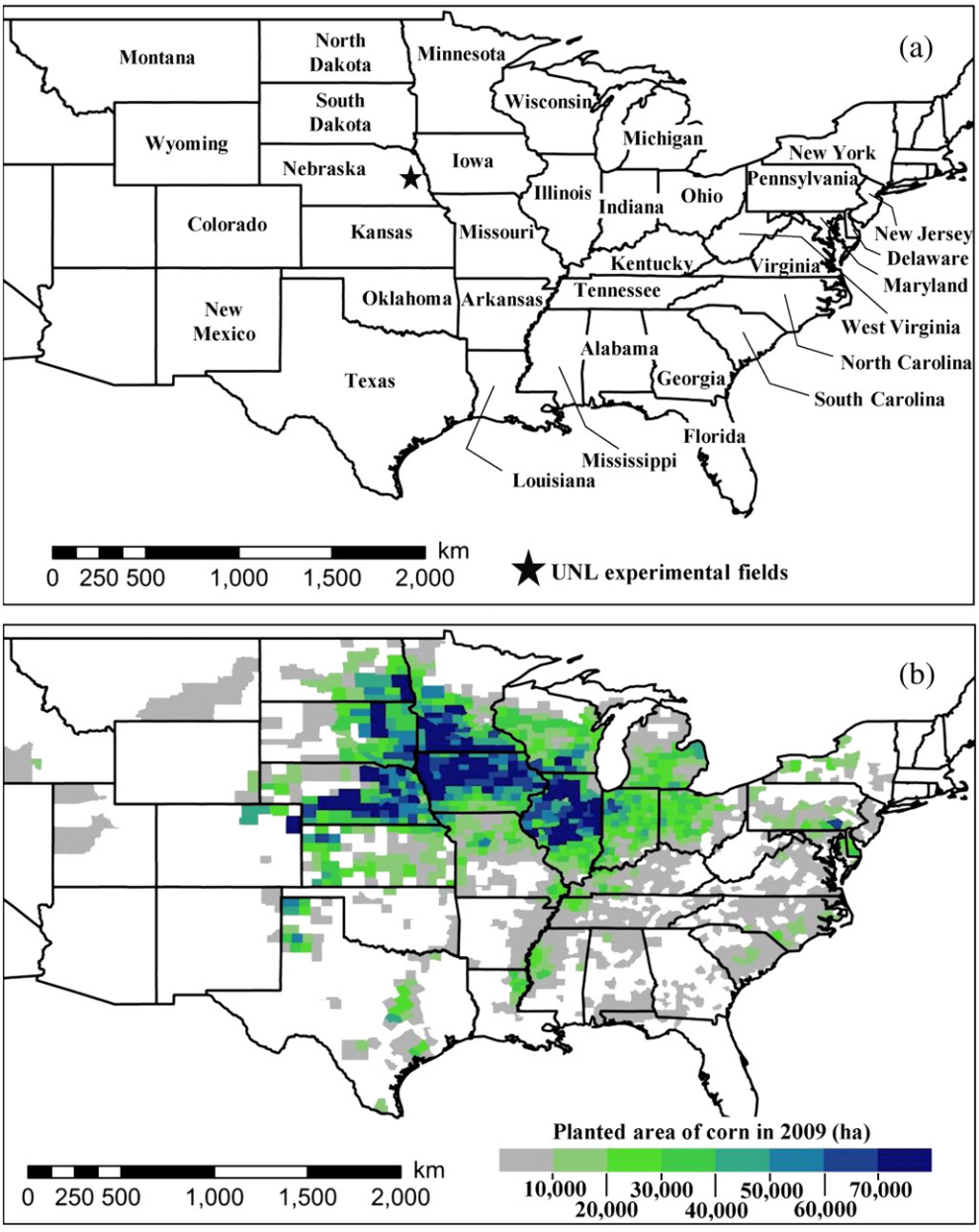

Fig. 1. Map of USA with location of the study states and UNL experimental fields (a). Corn-planted area derived from USDA/NASS in 2009 at a county level (b).

The spatial resolution of the original products of NASS-CDL varied from year to year owing to different data sources being used. The NASS-CDL used as representatives of 8 years (2000–2005, 2010, and 2011) were obtained from Landsat/TM with 30 m resolution. Those used as representatives of 4 years (2006–2009) were obtained from Resourcesat-1/AWiFS with 56 m resolution. The map projection of NASS-CDL was converted from Universal Transverse Mercator to MODIS sinusoidal projection. The percentage of corn area was calculated for each MODIS 250 m pixel.

3.3. NASS-Crop progress report

USDA/NASS surveys crop progress and condition based on questionnaires returned from more than 5000 reporters and publishes percent complete (area ratio) of crop fields that have either reached or completed a specific phenological stage, on ASD or state level, in a weekly report called the Crop Progress Report (NASS-CPR). Although the state level phenology information is available in the USDA/NASS Quick Stats 2.0 database with specific keywords (e.g., "corn-progress, silking, measured in pct"), the data are limited to 18 major corn producing states. In addition, the database does not reproduce all records contained in the original NASS-CPR. Therefore, the unrecorded data were complemented by checking the digital archive file (pdf or txt format) of state-level weekly reports, although the available back numbers of state level NASS-CPRs were different depending on state (e.g., Tennessee released only the past year (2011), whereas Mississippi released data for nearly a half-century. The last access date was July 31, 2012). The weekly data of percent complete (area ratio) were linearly interpolated to calculate the median date of target phenological stages (emerged, silking, dent, and mature stages), which was equivalent to the date when the interpolated percent complete reached 50% on a state level. Then, the median phenological dates of the NASS-CPR were compared with the MODIS-derived estimates to validate the SMF method.

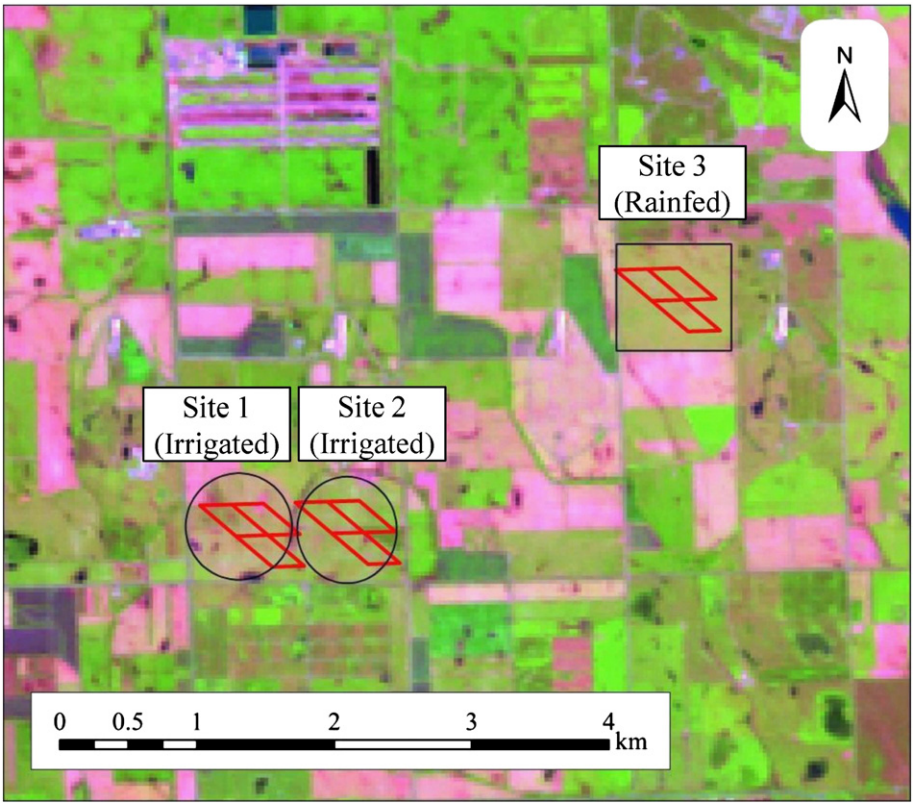

Fig. 2. MODIS-pixel footprints (red parallelograms) over experimental sites (two black circles and one black square) of the Carbon Sequestration Program at the University of Nebraska-Lincoln's Agricultural Research and Development Center in eastern Nebraska. The background picture is a false color image of Landsat 5 TM acquired on June 30, 2011. Band combination (R:G:B) is band 5:band 4:band 3. (For interpretation of the references to color in this figure legend, the reader is referred to the web version of this article.)

3.4. Ancillary corn grain yield data

The corn grain yield data were retrieved from the Quick Stats 2.0 database (last access date was May 19, 2012). The keywords selected as search criteria for the database were "SURVEY" for program, "CROPS" for sector, "FIELD CROPS" for group, "CORN" for commodity, "YIELD" for category, "CORN, GRAIN-YIELD, MEASURED IN BU/ACRE" for data item, and "COUNTY" or "STATE" for geographic level, respectively. The selected data period was from 2000 to 2011. The search results were exported to a text file in csv format. The text data were converted to a dbf file with ENVI/IDL (ExelisVIS: Exelis Visual Information Solutions, Boulder, Colorado, U.S.). Finally, they were spatially visualized with ArcGIS (ESRI: California, U.S.). The unit system for corn grain yield was converted from "bushel per acre (bu/ac)" to "ton per hectare (t/ha)."

3.5. Ground based observation data

At the UNL experimental fields (black star in Fig. 1a, black circles and square in Fig. 2), plant sampling was periodically conducted to record seasonal changes in the biophysical parameters of corn. Sites 1 and 2 were severely damaged by a hailstorm on September 13 [DOY: 256] 2010; thus, plant sampling was not conducted during the reproductive stage after the disaster in 2010. Observations of the crop phenological stages were conducted by agronomists once every 3–10 days. This study used the data observed from 2003 to 2011 to verify the accuracy of the SMF method at field scale (note: the occurrences of corn-R6 stage on site 1 in 2010 and site 2 in 2003 and 2010 were not recorded). Along with the previous studies (Sakamoto et al., 2010, 2011), this study estimated the crop developmental stages as target phenological stages on the same fields. The target crop developmental stages were early vegetative stage (V2.5) when the second or third leaf is fully expanded, silking stage (R1), dent stage (R5), and maturity stage (R6).

As for biophysical parameters, sampled leaves were divided into "green leaves", comprising all green leaf material from the collar to the leaf tip of destructive samples, and "dead leaves", which consist of greater than 50% necrotic (or entirely yellow) leaf. Then, the green leaf area (in m^2) was measured with a leaf area meter (model LI-3100, LI-COR: Lincoln, Nebraska, U.S.) to calculate the green leaf area index (green LAI in m^2/m^2) from the number of destructive samples and plant population density (unit: plants/m^2). Corn grain yield was calculated from the total weight of corn grains, which was gathered with a combine harvester for the whole field area, and was adjusted to 15.5% moisture content by grain moisture of each load (Verma et al., 2005). The corn grain yield observed in 2010 (site 1: 2.1 t/ha, site 2: 4.7 t/ha) was much lower than for other years (site 1: 10.5–13.5 t/ha, site 2: 12.5–14.2 t/ha, site 3: 7.7–12.0 t/ha) because of hailstorm damage. Therefore, these outlying observations were not used for model calibration of field-scale investigations.

4. Shape Model Fitting (SMF) method for detecting corn phenological stages

In this study, the MODIS-based crop phenology detection method called "Two-Step Filtering approach for detecting maize phenology" (TSF method, Sakamoto et al., 2010) was modified. The first modification was the use of MODIS WDRVI ($\alpha = 0.1$) as a proxy of corn green LAI, instead of WDRVI ($\alpha = 0.2$), based on the new findings. Guindin-Garcia et al. (2012) found that MODIS WDRVI ($\alpha = 0.1$)

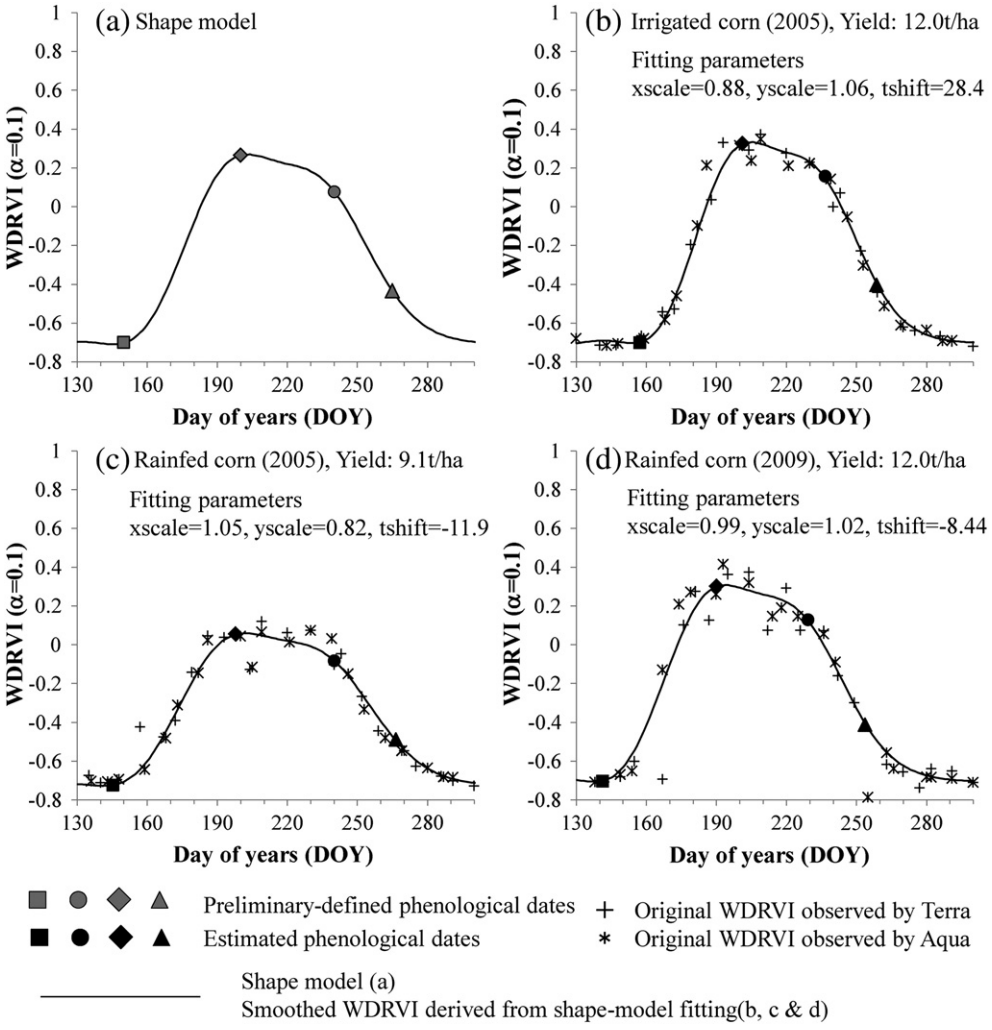

Fig. 3. Preliminary-defined "shape model" of corn growth based on MODIS WDRVI ($\alpha = 0.1$) (a). Smoothed profiles of WDRVI for the irrigated (b) and rainfed corn fields (c & d) were derived by shape-model fitting method using 8-day composite MODIS WDRVI ($\alpha = 0.1$) of Terra and Aqua. Three fitting parameters (xscale, yscale and tshift) are used in geometric transformation to fit the shape model on 8-day composite MODIS WDRVI ($\alpha = 0.1$) observations.

had a stronger linear relationship with corn green LAI than MODIS WDRVI ($\alpha = 0.2$). The second modification was omitting the smoothing of input time series VI data based on a wavelet-based filter from the preprocessing scheme. This was mainly because the wavelet based filtering algorithm required tremendous computation time and data storage if calculating all MODIS pixels for a continent wide area with 250 m resolution over 12 years. The third modification was to use both MODIS/Terra and MODIS/Aqua products in order to increase the observation frequency of the input time

Table 1
Accuracy assessment of the estimated phenological dates based on root mean square error (RMSE), correlation coefficient (r), and coefficient of variation (CV) when compared with ground-based observations obtained in the UNL experimental fields.

Phenological stage	r	RMSE (days)	CV (%)	n
Vegetative stage (V2.5)	0.77	4.5	3.0	20
Silking stage (R1)	0.80	3.2	1.6	20
Dent stage (R5)	0.47	9.0	3.8	20
Mature stage (R6)	0.85	4.7	1.8	17

n is the number of the comparison data.

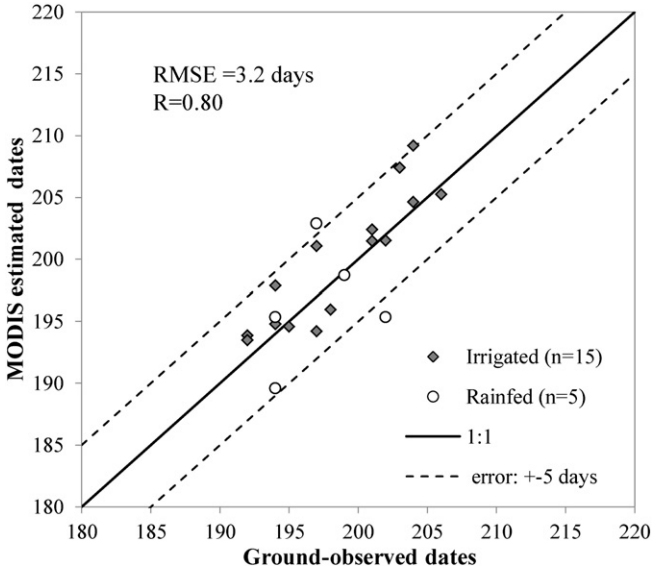

Fig. 4. MODIS-derived and ground-based observations of corn silking date (R1) planted on the UNL experimental fields.

series data. In this study, we call this modified crop phenology detection method the "Shape-Model Fitting method (SMF)" to emphasize its main feature (shape-model fitting scheme) and to distinguish it from the method that used the wavelet based filter. The calculation procedure of the SMF method is briefly explained as follows.

4.1. Shape model development

A shape model (Fig. 3a), which represents an abstract pattern of corn growth in terms of time-series WDRVI ($\alpha = 0.1$), was defined using the same procedure as in Sakamoto et al. (2010). Firstly, the shape model was defined by averaging 8 years (2001 to 2008) of daily smoothed WDRVI ($\alpha = 0.1$) observations from the irrigated continuous corn field (site 1 in Fig. 2). The relative locations of the key phenological stages on the shape model were empirically determined by reference to the ground-based phenology observations, and the preliminarily defined dates of key phenological stages were defined ($x_{0:V2.5}$ = DOY 150; $x_{0:R1}$ = DOY 200; $x_{0:R5}$ = DOY 240; $x_{0:R6}$ = DOY 265).

4.2. Fitting the shape model on observed time series WDRVI ($\alpha = 0.1$) data and estimating phenological date using scaling parameters

The shape model was geometrically scaled by Eq. (2), and then fitted on 8 day time series WDRVI ($\alpha = 0.1$) data observed by MODIS/Terra and MODIS/Aqua (Fig. 3b–d).

$$h(x) = yscale \times \{g(xscale \times (x + tshift)) + 0.8\} - 0.8 \quad (2)$$

where the function $g(x)$ refers to the preliminarily defined shape model (Fig. 3a). The function $h(x)$ is transformed from the shape model $g(x)$ in time- and VI-axis directions with the scaling parameters *xscale*, *yscale*, and *tshift*.

The scaling parameters were automatically optimized by using a functional subprogram named "CONSTRAINED_MIN" in the commercial programming language Interactive Data Language (IDL: Exelis

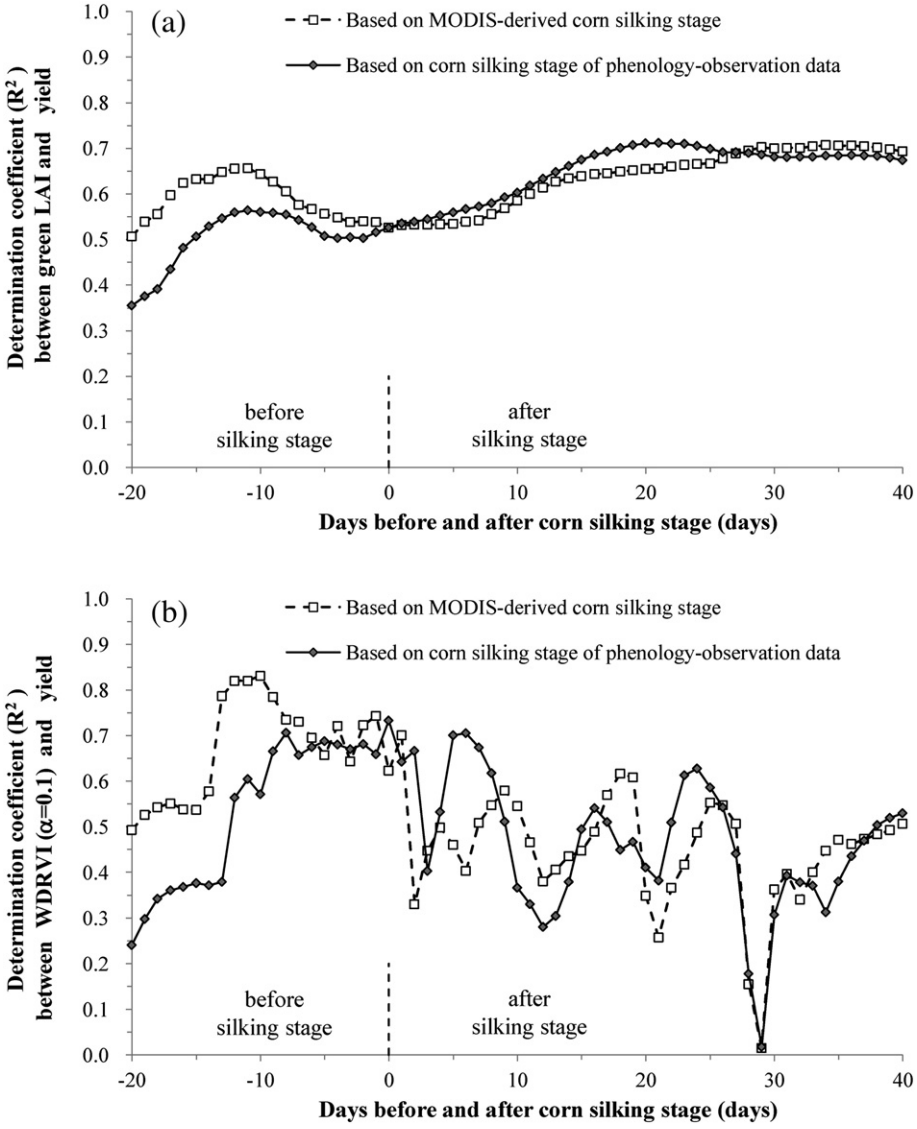

Fig. 5. Determination coefficient of the relationship between green LAI and yield (a) and WDRVI ($\alpha = 0.1$) and yield (b) plotted versus days before and after corn silking stage. The silking dates derived from ground-based observations (dark diamonds) and those estimated by the SMF method using time-series MODIS data (white squares) were separately used as time reference numerically defining crop phenological stage for comparison.

Visual Information Solutions, Boulder, Colorado, U.S.). The optimization criterion was the discrepancy score (DS_{MODEL}) between the rescaled shape model $h(x)$ and observed time series WDRVI ($\alpha = 0.1$) $f(x)$.

$$DS_{MODEL} = \sqrt{\frac{1}{n}\sum_{t=t_0,t_1\ldots t_n}(f(t)-h(t))^2} \quad (3)$$

where n is the number of available WDRVI ($\alpha = 0.1$) observations of MODIS/Terra and Aqua, excluding cloud covered pixels, that were defined by a reflectance value greater than 0.2 in the blue band. t is the actual observation date recorded in the DOY layer of MOD09A1 and MYD09A1. If the observation dates (t_a) of MODIS/Terra and MODIS/Aqua are coincident in a given 8-day period, the WDRVI ($\alpha = 0.1$) with a lower reflectance value in blue band is selected as an observed WDRVI ($\alpha = 0.1$) for that period: $f(t_a)$.

The scaling parameters were obtained for each pixel, as shown in the case examples of irrigated and rainfed fields (Fig. 3b–d). Because it is possible to reversely duplicate daily smoothed profiles of WDRVI ($\alpha = 0.1$) by substituting the three scaling parameters (*xscale*, *yscale*, and *tshift*) into Eq. (2), the SMF method was expected to have the advantage of saving disk space. If the focus was not on local changes of time series VI data, it was not necessary to record large volumes of smoothed VI data on a daily basis.

This study used the rescaled shape model $h(x)$ as daily smoothed WDRVI ($\alpha = 0.1$), and compared it with green LAI and final corn grain yield. Finally, the MODIS-based phenological dates were estimated by substituting the optimized scaling parameters and the preliminarily determined dates of key phenological stages ($x_{0:V2.5}$ = DOY 150; $x_{0:R1}$ = DOY 200; $x_{0:R5}$ = DOY 240; $x_{0:R6}$ = DOY 265) into the following conversion equation.

$$x_{est} = xscale \times (x_0 + tshift) \quad (4)$$

where *xscale* and *tshift* are the scaling parameters derived from the shape model fitting scheme and x_{est} is an estimate of the key phenological date.

For validation of the SMF-derived key phenological dates on a regional scale, the MODIS 250 m pixels within which corn coverage area (area ratio) was over 95% were selected for the purpose of comparison with the estimation results of the previous study on an ASD level (Sakamoto et al., 2011). After estimating each phenological date at pixel level, state median values were calculated for comparison with the NASS-CPR derived statistics.

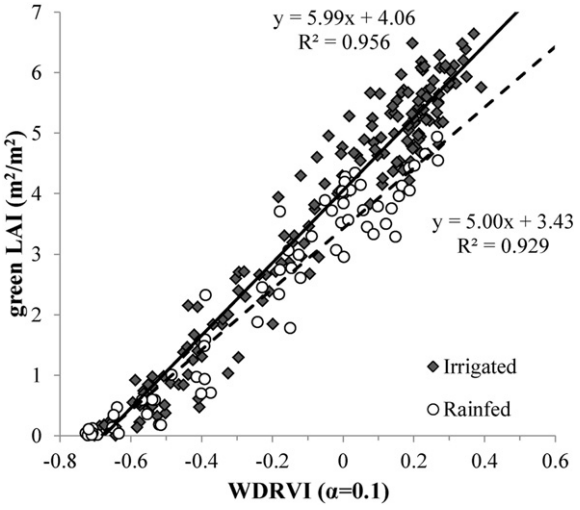

Fig. 6. Green LAI versus MODIS WDRVI ($\alpha = 0.1$), derived from the shape model fitting method for irrigated and rainfed corn fields.

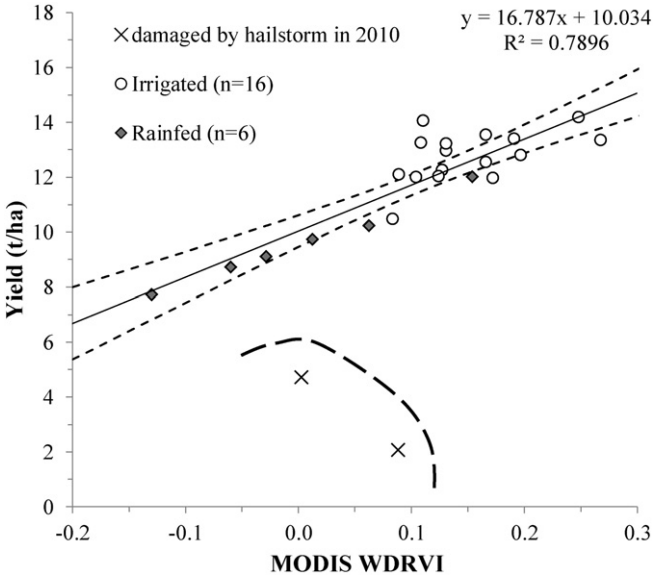

Fig. 7. Comparison between corn grain yield and smoothed MODIS WDRVI ($\alpha = 0.1$), observed 10 days before estimated silking date at a field scale.

5. Calibration and validation of corn grain yield estimation model on a field scale

5.1. MODIS-derived key phenological dates on a field scale

The SMF method was applied to the three MODIS pixels within each experimental site in Mead, Nebraska (Fig. 2). Then, the estimated phenological dates were averaged at each site for comparison with the ground-based phenology observations (Table 1). The SMF method yielded the best result for the R1 stage (RMSE = 3.2 days), which was comparable to the original method (RMSE = 2.4 days: Sakamoto et al., 2010). Coefficient of variation (CV) for R1 stage dates for the rainfed site (2.3%) was larger than that of the irrigated sites (1.3%). The SMF method was able to estimate the R1 dates for 17 of 20 samples (85% of all observations) with a margin of ±5 days (Fig. 4). Considering that NASS-CPR, which had been the sole reliable source of phenology information, represents the overall trend of crop growth status on a regional scale of ASD or state level, the SMF method did provide high

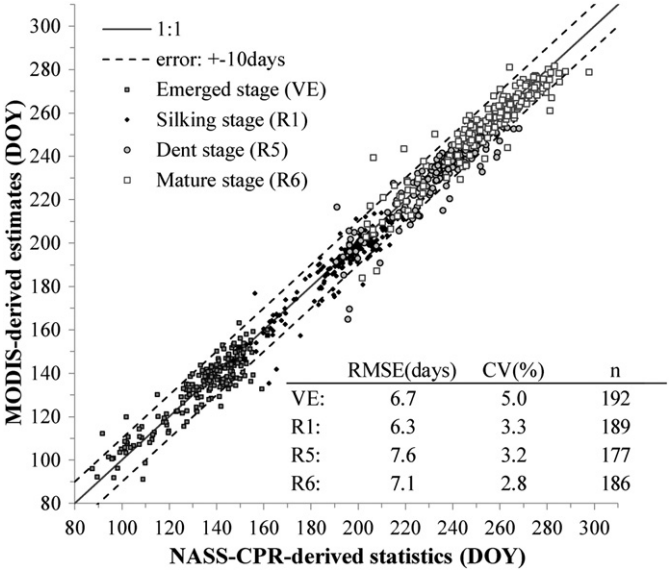

Fig. 8. MODIS-derived estimates of key phenological dates plotted versus the NASS-CPR statistics.

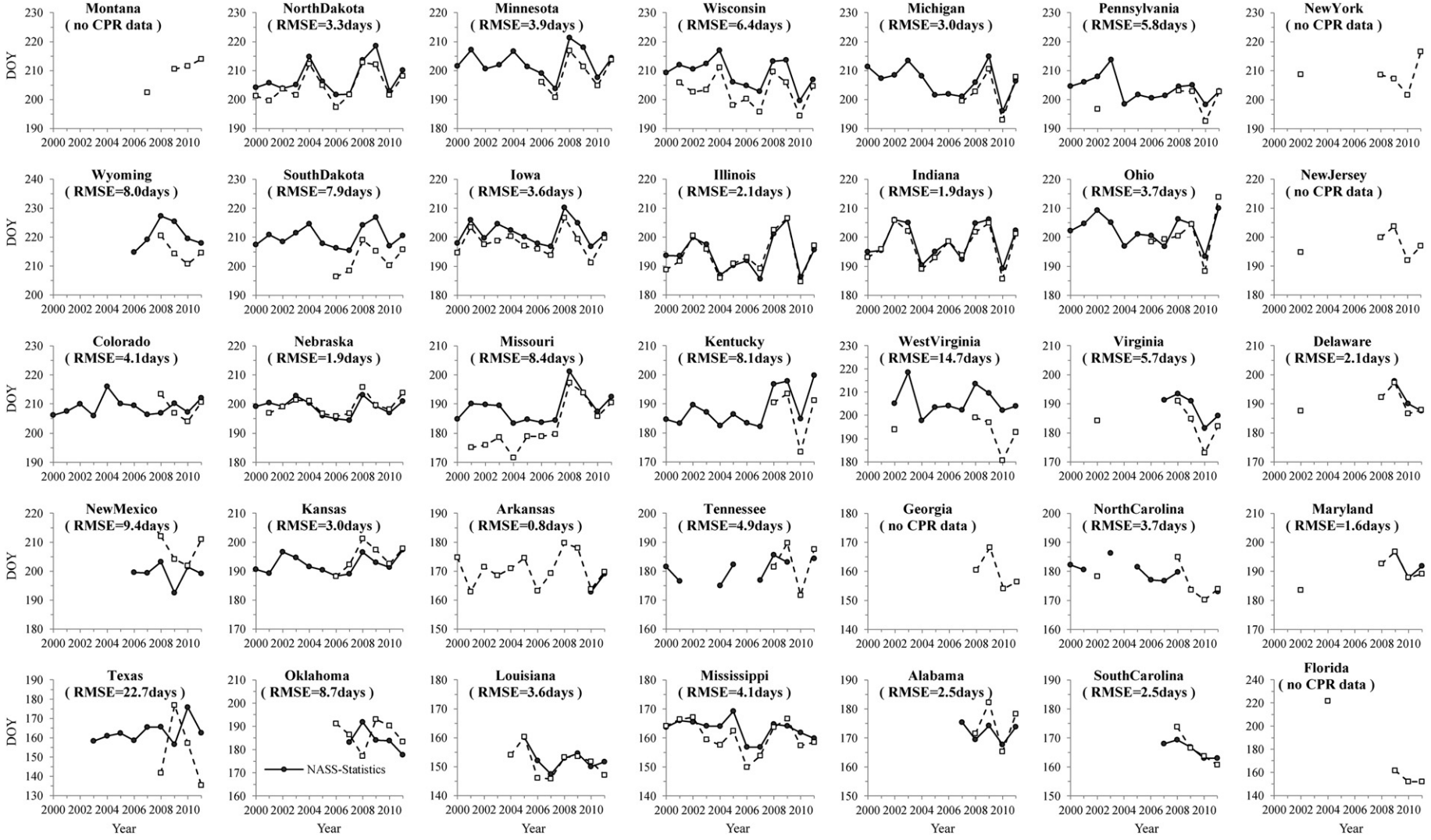

Fig. 9. MODIS-derived estimates of corn silking dates (squares) and the statistics (circles) at a state level.

resolution quantitative information on crop phenological stages with reasonable accuracy.

5.2. Relationships of final corn grain yield with green LAI and MODIS WDRVI ($\alpha = 0.1$)

Guindin-Garcia (2010) found that there was a strong correlation between final corn grain yield and green LAI, especially during the mid-grain filling period (R3: milk stage to R4: dough stage). Using the same data source of corn biophysical parameters, but for a longer observation period (2001–2011), we investigated again the most sensitive phenological stage at which green LAI has the highest linear correlation with the final corn grain yield. This study defined the date of corn silking stage (R1) as the origin of the time dimension when numerically specifying the crop phenological stage. The reason why the R1 stage was used as the time reference was that the SMF method is able to estimate R1 dates with the highest accuracy. Firstly, green LAI observed at irregular time intervals were linearly interpolated to generate time series data of green LAI on a daily basis. Then, determination coefficients (R^2) between corn grain yield and the linearly interpolated green LAI were calculated in time period 20 days before the R1 stage to 40 days after the R1 stage. This study used both ground-based phenology observations and SMF-estimated R1 dates for temporal standardization of the phenological stage, and investigated the effect of the difference in the temporal standardization on the temporal feature of linear correlation between them.

Using the date of ground-based R1 stage observations (black diamonds in Fig. 5a), this study reached the same result as Guindin-Garcia (2010), namely, that green LAI during the reproductive stage (about 20 days after R1 stage) showed stronger correlation than that during the vegetative stages (before R1 stage). However, using the SMF-estimated R1 dates (white squares in Fig. 5a), the temporal feature of the R^2 showed a clear local peak during the vegetative stage (11 days before R1 stage). The temporal standardization based on the SMF-estimated R1 dates may have the potential to improve the performance of a corn grain yield estimation model aimed at early yield prediction using an indicator observed around the late vegetative stage.

In Fig. 5b, corn grain yield was compared with linearly-interpolated MODIS WDRVI ($\alpha = 0.1$). The temporal feature of R^2 based on MODIS

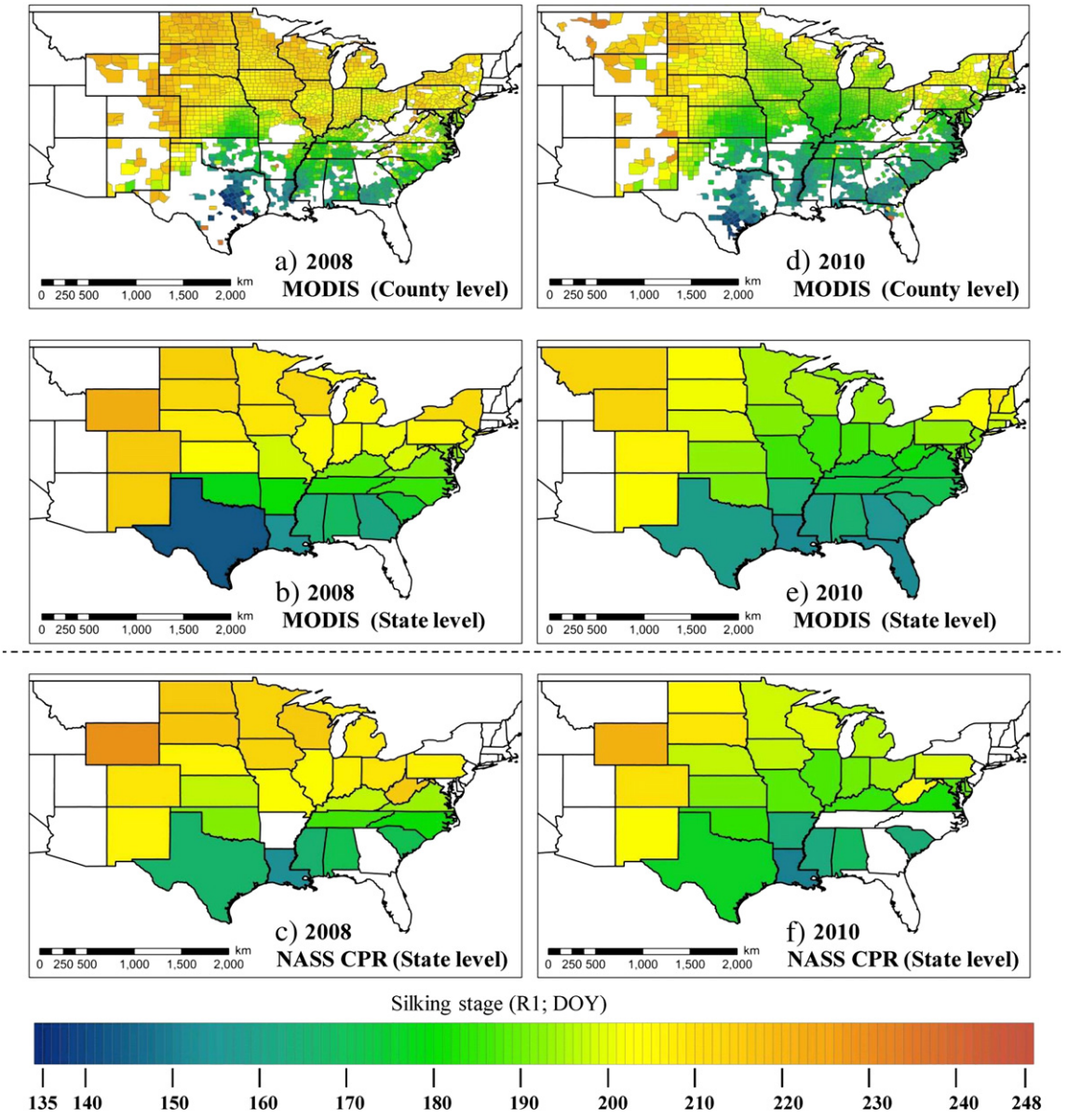

Fig. 10. Spatial distribution of corn silking dates in 2008 and 2010: the MODIS-derived estimations at county level (a, d) and state level (b, e); the NASS-CPR-derived statistics on a state level (c, f).

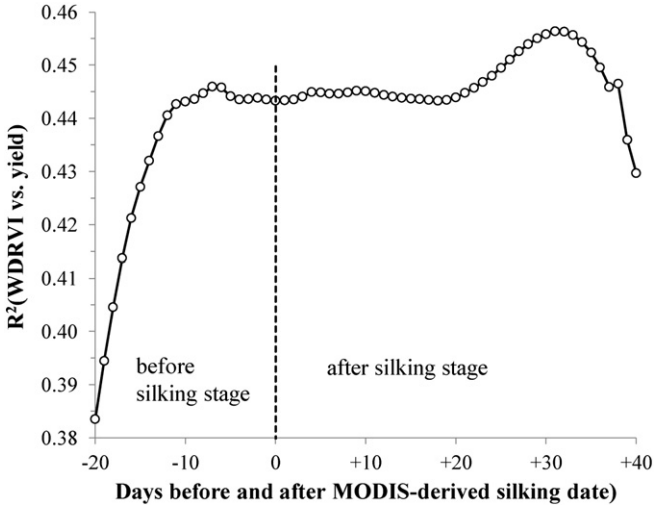

Fig. 11. Determination coefficient of the linear relationship between county-averaged MODIS WDRVI ($\alpha = 0.1$) and county-averaged yield observed before and after the SMF-estimated silking date.

WDRVI ($\alpha = 0.1$) (Fig. 5b) had similar characteristics to those based on green LAI (Fig. 5a) during the vegetative stage. The temporal feature, which was temporally standardized by the SMF-estimated R1 dates (white squares in Fig. 5b), also showed a local maximum peak at 10 days before the R1 stage that was higher than the peak temporally standardized by the ground observed R1 dates (black diamonds in Fig. 5b). Furthermore, the local maximum of R^2 between MODIS WDRVI ($\alpha = 0.1$) and corn grain yield ($R^2 = 0.83$) was higher than that based on the ground observed green LAI ($R^2 = 0.66$). In addition, it was found that MODIS WDRVI ($\alpha = 0.1$), observed during the reproductive stage (after the R1 stage) had a lower correlation with the corn grain yield than that during the vegetative stage regardless of the time reference (Fig. 5b). This temporal feature was in contrast to the case using the linearly interpolated green LAI as an explanatory variable. This is probably because the sensitivity of MODIS WDRVI ($\alpha = 0.1$) to green LAI is different before and after the R1 stage owing to a morphological change in the crop community (leaf angle distribution, leaf chlorophyll content, leaf necrosis, and so on). In addition, a probable cause of the reduced sensitivity after the R1 stage is the difference in plant population density between the irrigated and rainfed fields. The rainfed corn was always planted with a lower plant population density (5.02–6.05 plants/m^2) than the irrigated fields (6.92–8.25 plants/m^2). The difference in plant population density and water stress may create a difference in overlapping leaf area between the irrigated field and the rainfed field, especially when the vegetation fraction reaches its maximum; accordingly, the slope of the linear best fit function of the relationship between MODIS WDRVI ($\alpha = 0.1$) and green LAI in the rainfed field was lower than that in the irrigated field (Fig. 6). Thus, for the same green LAI, WDRVI ($\alpha = 0.1$) was higher in rainfed fields than in irrigated fields, indicating greater absorption ability of rainfed corn planted sparsely.

The saw tooth profiles observed in Fig. 5b were assumed to be due to various noises such as cloud cover and mixed pixel effects, which cannot be absolutely excluded in 8-day MODIS composite products. Therefore, this study used the smoothed MODIS WDRVI ($\alpha = 0.1$), derived from the SMF method, to reduce the effect of these noises on the estimation of final corn grain yield in the proposed model. Considering the temporal features observed in Fig. 5b, this study defined smoothed MODIS WDRVI ($\alpha = 0.1$) observed before the SMF derived R1 stage as an explanatory variable for the MODIS-based yield estimation model. Fig. 7 shows high performance of the field scale yield estimation model, which was able to estimate the corn grain yield with RMSE = 0.81 t/ha, coefficient of variation, CV = 6.8%, and mean

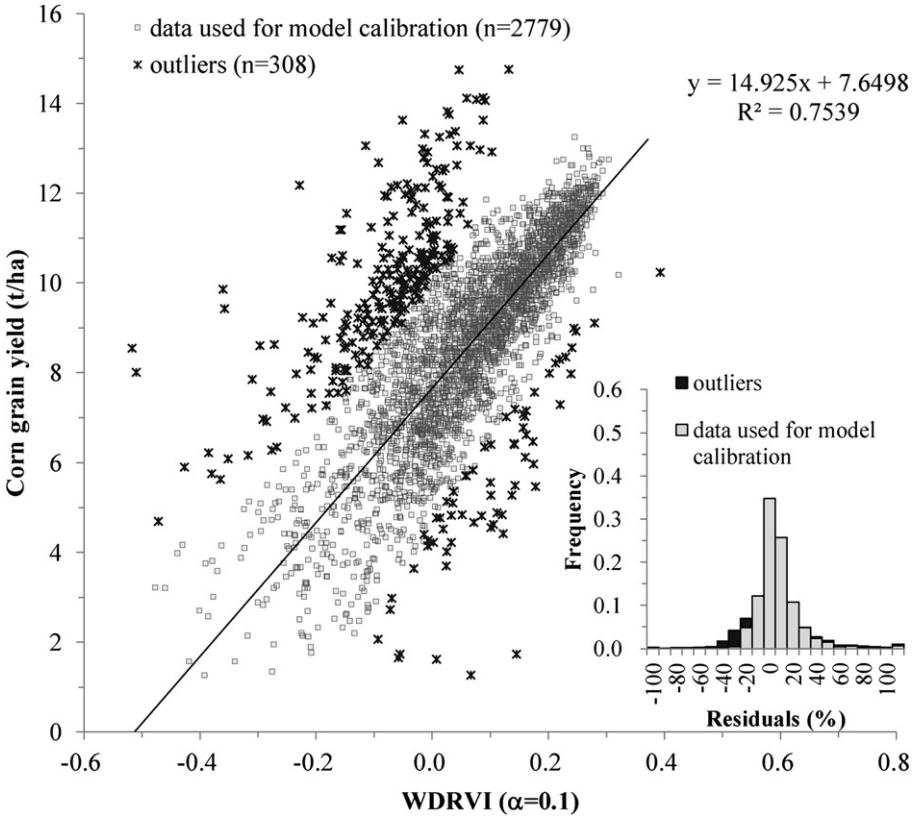

Fig. 12. Model calibration for regional scale. Corn grain yield at county level in 2009 and 2010 plotted versus WDRVI ($\alpha = 0.1$) at 7 days before MODIS-estimated silking stage.

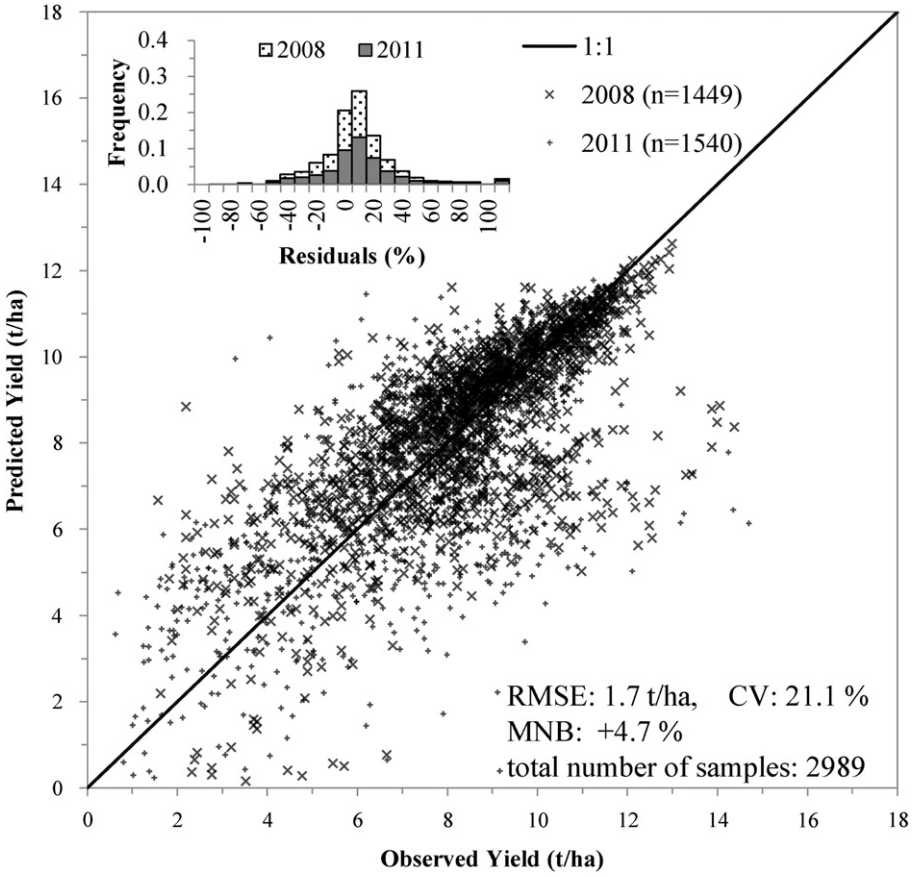

Fig. 13. Model validation at regional scale. WDRVI ($\alpha = 0.1$) taken 7 days before MODIS-estimated silking stage versus corn grain yield observed at county level in 2008 and 2011.

normalized bias, MNB = +0.5%; exceptions are the two crops that were damaged by the local hailstorm in 2010 (× marks in Fig. 7).

As a matter of course, we considered it difficult to assess harvest failure caused by meteorological disasters or pest and insect damage during the reproductive stage. It was also noticed that the model had a good linear relationship with rainfed corn grain yield, although all rainfed data points were distributed under the approximate line on the scatter diagram (gray diamonds in Fig. 7). Given that crop cultivation method was not considered in the corn yield estimation model, the lower plant population density of the rainfed field may be related to this distribution, which may cause a bias error when directly applying this field scale yield estimation model to a wide region.

6. Model for estimating corn grain yield at regional scale

6.1. Validation of the SMF-derived key phenological dates on a regional scale

The SMF method gave the best performance for detecting the R1 stage with the lowest RMSE when scaling up the study area from field to state level (Fig. 8), which was comparable to the previous studies detecting ASD-level phenological stages (Sakamoto et al., 2010, 2011). Fig. 9 shows comparison of the median dates of the corn R1 stage estimated by SMF and the NASS-CPR derived statistics. The estimation accuracy (RMSE) varied from state to state. The annual variations of the SMF-estimated phenological dates matched well with those of NASS-CPR derived statistics, except for several states. However, the results indicated the existence of a certain bias error in the SMF derived estimates, especially for Wisconsin, Kentucky, South Dakota, North Dakota, Minnesota, Iowa, Wyoming, West Virginia, and Virginia.

Although the SMF-derived estimates were affected by a mixed-pixel effect caused by the spatial pattern of cropping intensity, there is also another possibility that the NASS-CPR includes some bias error. Sakamoto et al. (2011) conducted a detailed validation of the MODIS derived estimate on an ASD level and then suggested the possibility that the bias errors (ca. +5 days) were included in the NASS derived R1 stage in Iowa, but not Illinois. County median dates of the SMF-estimated R1 stage were also calculated to visualize the detailed spatial distribution of corn phenology all over the U.S. Fig. 10a–f panels are clear examples of a late planting year (2008) and an early planting year (2010), respectively. The continuous spatial variations of crop phenology are much easier to understand from the SMF-derived phenology maps (Fig. 10a, d) than the NASS-CPR derived statistics (Fig. 10c, f). The spatio-temporal features of the R1 stage were considered to reflect differences in planting season. The county-level phenology maps suggested that the corn R1 stage began in the southern states with warm climate, spreading to the northwest states with cold climate. Several counties with anomalous values of the R1 stage were located in Wyoming, Colorado, New Mexico, and Texas (Fig. 10a, d), which are outlying regions of the U.S. Corn Belt. The mixed-pixel effect due to a limited number of available corn pixels was cited as a possible cause of the anomalous values on the county-level phenology maps.

6.2. Calibration and validation of corn grain yield estimation model for a regional scale

The MODIS data and the USDA/NASS county-level statistics, obtained from 2009 and 2010 were used for model calibration. The target MODIS 250 m pixels were selected by an area ratio threshold of 95% (i.e., over 95% of a 250 m pixel's area was occupied by corn).

Table 2
Accuracy assessment of the MODIS-estimated corn grain yield against NASS derived statistics of 2008 and 2011 on a county level. The states were rearranged in ascending order of CV to form two groups (A: good estimation performance, and B: poor estimation performance) for Fig. 15.

State	CV (%)	RMSE (days)	n	Group
Iowa	6.3	0.65	198	A
Illinois	7.0	0.71	195	
Delaware	9.1	0.69	6	
Minnesota	10.1	0.96	143	
Ohio	10.8	0.97	149	
West Virginia	12.5	0.99	15	
Wisconsin	12.7	1.10	121	
Michigan	12.8	1.06	114	
Indiana	12.8	1.17	173	
Nebraska	13.5	1.33	172	
Kentucky	16.4	1.33	138	
New York	16.9	1.41	80	
South Dakota	18.1	1.36	115	
Missouri	20.4	1.59	151	
Pennsylvania	21.3	1.56	90	
Tennessee	21.5	1.61	91	
New Jersey	23.5	1.71	24	
Maryland	24.0	1.72	38	
Mississippi	24.8	1.88	61	B
Alabama	24.9	1.64	38	
North Dakota	27.4	1.69	83	
Louisiana	27.7	2.30	35	
Wyoming	31.0	2.62	11	
Arkansas	31.9	2.91	54	
North Carolina	32.3	1.80	131	
Montana	32.9	2.97	9	
Kansas	33.5	2.21	137	
Virginia	37.0	2.41	84	
Georgia	42.3	3.71	81	
Colorado	43.2	3.46	39	
Texas	48.9	2.68	107	
Oklahoma	51.4	2.51	35	
New Mexico	52.7	5.53	3	
South Carolina	54.7	2.18	53	
Florida	–	–	–	

The area ratio threshold of 95% was empirically determined to limit the influence of the mixed-pixel effect on area averaged WDRVI ($\alpha = 0.1$) with due consideration to the available MODIS pixel count in a region that is not heavily cultivated with corn. Fig. 11 shows the temporal features of the determination coefficient of the linear relationship between the county-level corn grain yield and the county averaged MODIS WDRVI ($\alpha = 0.1$), observed on a given day before and after the SMF-estimated R1 dates. It was found that there was a small peak of sensitivity around 7 days before the MODIS-estimated R1 stage, as was found at the field scale investigation. In addition, there was also a higher R^2 peak during the reproductive stage (around 31 days after the MODIS-estimated R1 stage).

The determination coefficient on a county level during vegetative stage was much lower ($R^2 = 0.445$) than that obtained in the investigation at a field scale ($R^2 = 0.790$, Fig. 7). This was because many outliers were included in the scatter plot made from the calibration dataset (Fig. 12), which perturbed the determination coefficient when making a linear approximate equation. Therefore, the corn yield estimation model was calibrated through the following steps. Firstly, the timing of the MODIS WDRVI ($\alpha = 0.1$) used as an explanatory variable was fixed at 7 days before the SMF-estimated R1 dates. Secondly, 10% of data plots (black asterisks in Fig. 12) were subjectively identified as outliers and automatically removed from the calibration dataset. As shown in the residual histogram (Fig. 12), the outliers potentially cause gross estimation errors of more than −20% or +30%. Finally, the following corn yield estimation model was determined by least square linear regression using the remaining 90% of data plots (gray squares in Fig. 12).

$$\text{Yield}\,(\text{t/ha}) = 14.925 \times \text{MODIS WDRVI}\,(\alpha = 0.1, \text{at 7 days before R1 stage}) + 7.6498. \quad (5)$$

The established regional scale yield estimation model (Eq. (5)) was applied for the validation dataset of MODIS observed in 2008 and 2011. Fig. 13 shows the comparisons between the MODIS-estimated corn grain yields and the statistics of USDA/NASS on a county level. The performance of the regional scale corn grain yield estimation model (RMSE: 1.7 t/ha, CV: 21.1%, MNB: +4.7%) was not as good as that obtained at the field scale (RMSE: 0.81 t/ha, CV: 6.8%, MNB: +0.5% in Fig. 7). The degradation of model performance at the regional scale was thought to be caused by the influence of mixed-pixel effects on the MODIS VI values. As will hereafter be described in detail, we did not expect the same level of accuracy for every county in the US, because the degree of the mixed-pixel effect may be affected by cropping intensity depending on location. According to the accuracy assessment for individual states, the estimation accuracy based on the coefficient of variance (CV) varied from 6.3% in Iowa to 54.7% in South Carolina (Table 2).

6.3. Spatio-temporal pattern of corn grain yield in the US

The MODIS-derived estimates (Fig. 14a) and the USDA/NASS derived statistics (Fig. 14b) were visualized to examine the yearly changes in spatial distribution of corn grain yield from 2000 to 2011. The reason why the MODIS-estimated spatial coverage was constrained from 2000 to 2007 is that the spatial coverage of the NASS-CDL data varied from year to year. The differences between them were also mapped to investigate the regional estimation error (Fig. 14c). The MODIS-derived estimates of spatial distribution were in excellent agreement with the USDA/NASS derived statistics, especially for high yield regions (more than 10 t/ha) in the U.S. Corn Belt extending over Minnesota, Michigan, Iowa, Indiana, Iowa, and Ohio. In addition, the regional scale yield estimation model was able to detect several isolated areas of poor yield, which included the southern and eastern regions of Indiana, the southeastern corner of Nebraska, the southern region of Illinois in 2002 (Fig. 14 a2 & b2), the southern region of Illinois in 2003 (Fig. 14 a3 & b3), the southern region of Illinois in 2007 (Fig. 14 a7 & b7), and the southern region of Iowa in 2010 (Fig. 14 a10 & b10).

As for the disagreement, the counties in which the corn yield was underestimated (sky blue/blue counties in Fig. 14c: more than 1.0 t/ha error) were intensively distributed around the following three regions in any given year. The first region was located in the High Plains, where the Ogallala Aquifer lies beneath portions of South Dakota, eastern Wyoming, Nebraska, eastern Colorado, Kansas, New Mexico, Oklahoma, and Texas (Wichelns, 2010). The underestimated counties in western Wyoming, Montana, and western Colorado are not above the Ogallala Aquifer; however, according to the high-resolution map of original NASS-CDL, most of the corn-cropped fields in western Wyoming and Montana are sparsely-distributed along branches of the Missouri River, and are probably irrigated by river water in these areas. The second region was located in the lower Mississippi river basin, especially along adjacent territories of Arkansas, Louisiana, Tennessee, and Mississippi. The third region was the southwestern region of Georgia. All three regions are widely known as well irrigated

Fig. 14. Maps of the MODIS-estimated corn grain yield (a0–a11) and the NASS-derived corn grain yield (b0–b11) at county level. The counties where corn grain yield was overestimated more than 1.0 t/ha or underestimated less than 1.0 t/ha, were also colored with the same scale map (c0–c11). (For interpretation of the references to color in this figure legend, the reader is referred to the web version of this article.)

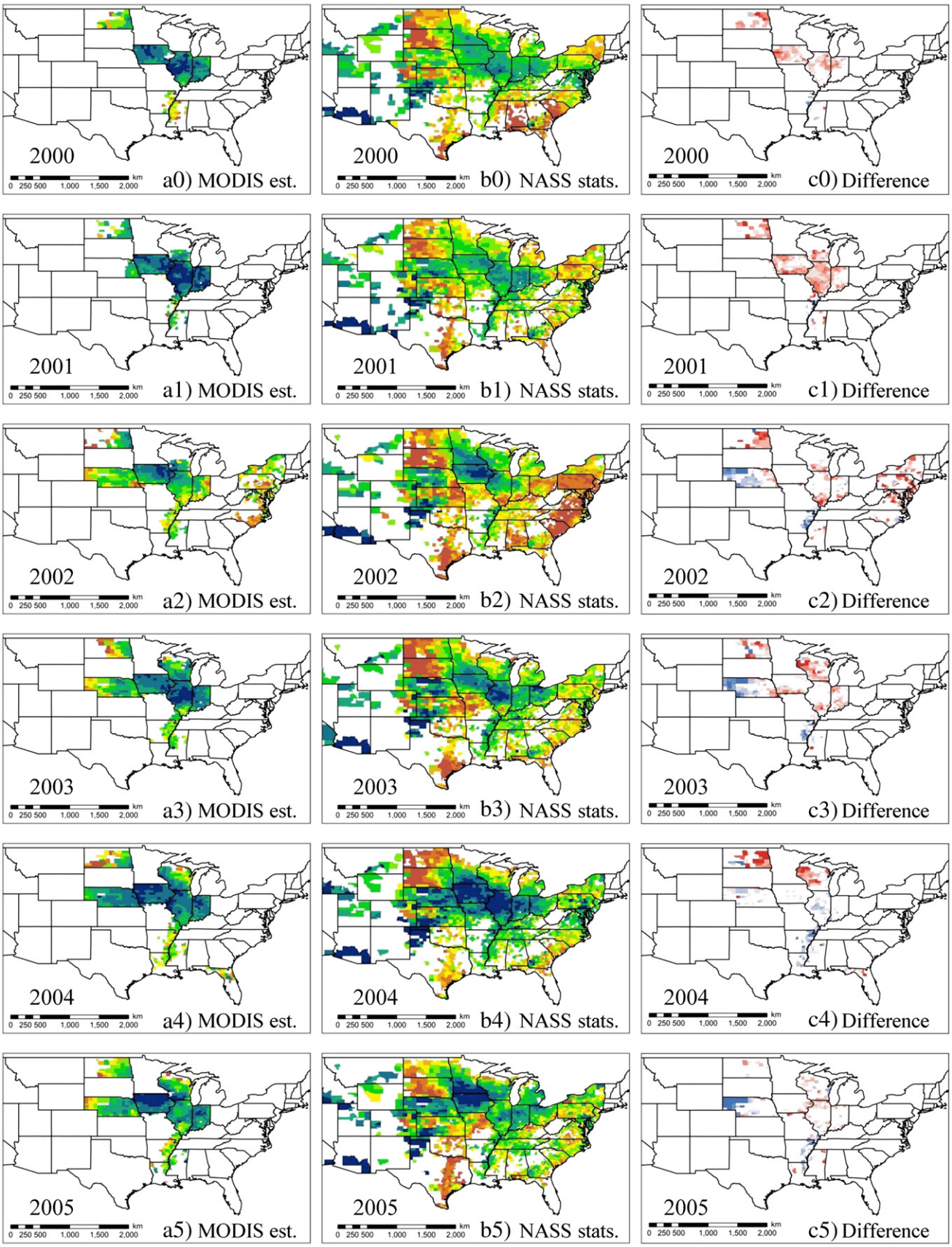
2000
a0) MODIS est.
2000
b0) NASS stats.
2000
c0) Difference
2001
a1) MODIS est.
2001
b1) NASS stats.
2001
c1) Difference
2002
a2) MODIS est.
2002
b2) NASS stats.
2002
c2) Difference
2003
a3) MODIS est.
2003
b3) NASS stats.
2003
c3) Difference
2004
a4) MODIS est.
2004
b4) NASS stats.
2004
c4) Difference
2005
a5) MODIS est.
2005
b5) NASS stats.
2005
c5) Difference
0 250 500 1,000 1,500 2,000 km
Yield (t/ha)
4.0 5.0 6.0 7.0 8.0 9.0 10.0 11.0
Difference between MODIS estimates and NASS statistics(t/ha)
-3.0 -2.5 -2.0 -1.5 -1.0 -0.5 0.0 +0.5 +1.0 +1.5 +2.0 +2.5 +3.0

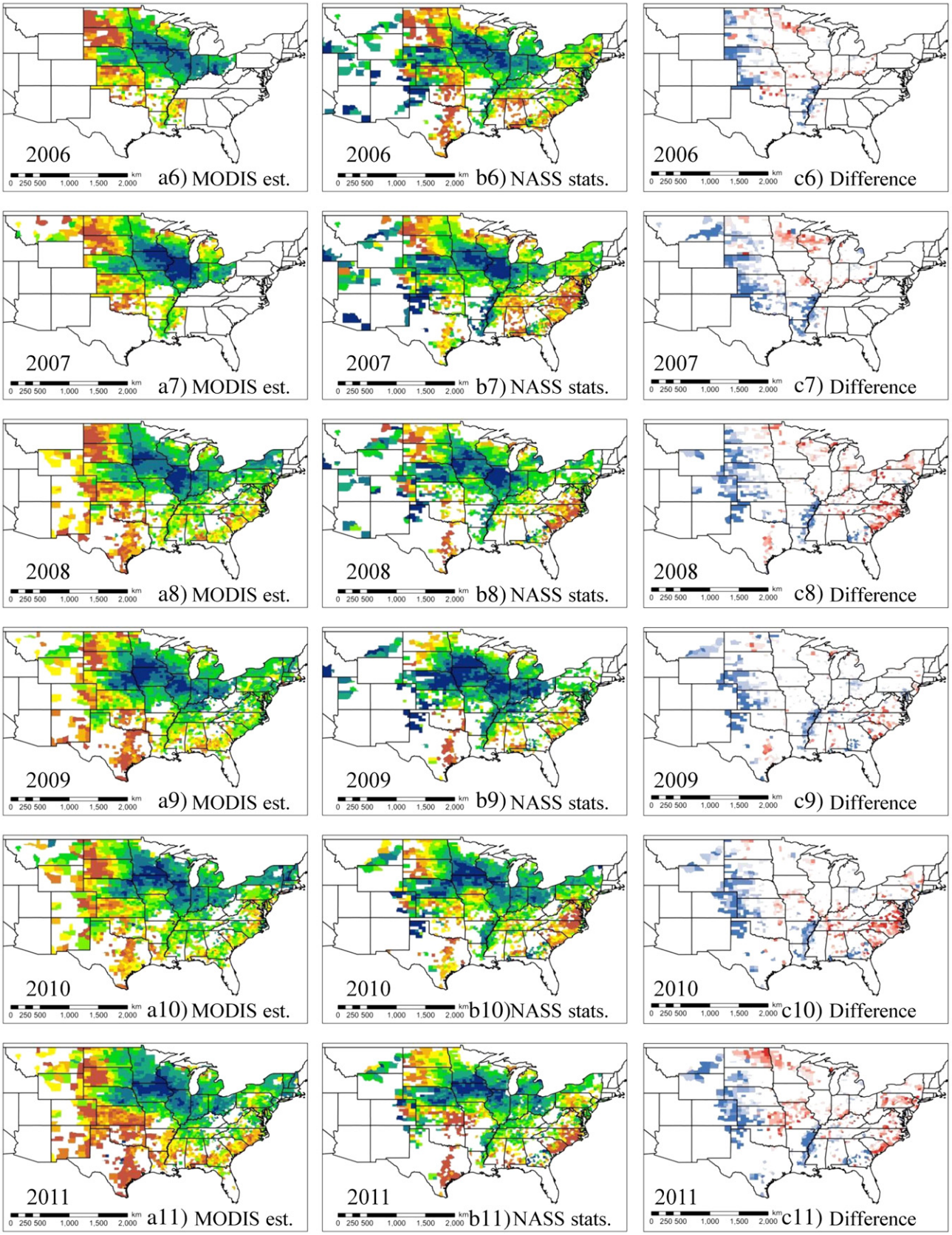

Fig. 14. (*continued*).

agricultural regions that take advantage of a major water resource. These locations agreed well with the MODIS-derived irrigation map made by Ozdogan and Gutman (2008). On the other hand, the counties for which the corn yield was overestimated (pink–red counties in Fig. 14c: more than 1.0 t/ha error) were located mainly in the states on the East Coast, North Dakota, Minnesota, Wisconsin, and Missouri. A possible reason of the underestimation and overestimation of corn grain yield is the mixed-pixel effect caused by surrounding land cover and land use, especially in regions where corn fields are sparsely distributed. When it comes to underestimation, mostly observed in major irrigated regions, MODIS pixels of irrigated corn fields, which cover a high-density plant community but also include the influence of surrounding non-irrigated fields or grassland owing to a variable footprint size caused by sensor view angle, are susceptible to the mixed-pixel effect resulting in lower MODIS WDRVI ($\alpha = 0.1$). In contrast, if target MODIS pixels of rainfed corn are surrounded by natural vegetation, such as forest, in a region of high rainfall, the mixed-pixel effect has the potential to increase the MODIS WDRVI ($\alpha = 0.1$) of the target pixels. There was another possible reason relating to a difference in plant population density. Some sites in western Nebraska have plant populations much lower than 30,000 plants/ha. According to the crop production report of USDA/NASS released on November 9, 2011, there was great variability in corn plant population, which ranged from 53,100 plants/ha in Kansas to 76,200 plants/ha in Iowa. As described in Section 5.2, a low plant population has the potential to cause bias error in the MODIS-based corn yield estimation model (Fig. 7).

6.4. Scaling up from field level to state level to validate yearly changes in yield estimations

The MODIS-derived yield estimates were scaled up from field level to state level to confirm the model applicability for state level yield estimation, which was calculated by a buildup approach from pixels to state wide regions. The MODIS-estimated corn grain yields were compared with the NASS derived statistics from 2000 to 2011 at state level (Fig. 15). Because the MODIS-estimated corn grain yield had a large margin of error depending on the location, the 35 states were divided into two groups (group A: high estimation accuracy; group B: low estimation accuracy) on the basis of the county level validation result (Table 2). As far as the 18 states of group A were concerned, the model could estimate state level corn grain yields with high accuracy (RMSE = 0.81 t/ha) over a wide range (approx. 6–11.5 t/ha). In contrast, the MODIS-estimated corn grain yield tended to be underestimated in the other 17 states of group B with an RMSE = 2.09 t/ha.

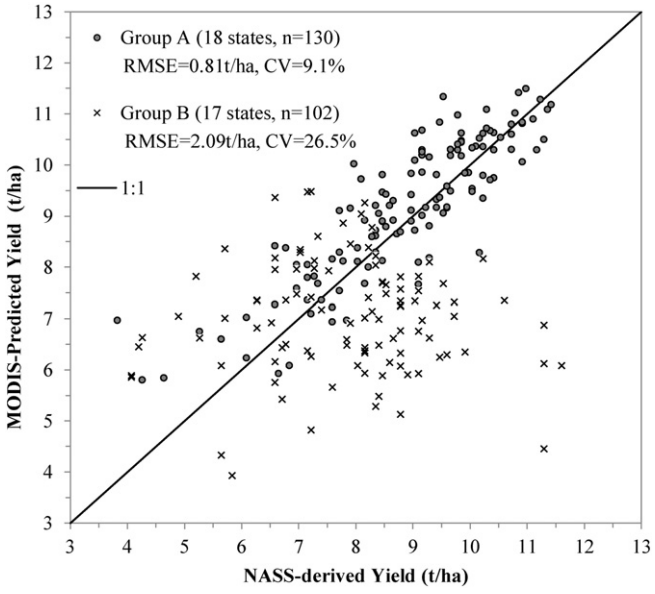

Fig. 15. Corn grain yield predicted by MODIS and the yield derived from NASS data from 2000 to 2011 at state level. The 35 states were divided into two groups on the basis of estimation accuracy obtained at the county-level model validation (Table 2 shows the grouping in detail).

Fig. 16 shows the yearly comparison of the state level corn grain yield between the MODIS-derived estimates and the USDA/NASS-derived statistics. Although the available data periods were different from state to state, the MODIS-estimated corn grain yields were in excellent agreement with the USDA/NASS derived statistics in terms of annual variation, especially in the top corn producing states, consisting of the U.S. Corn Belt (South Dakota, Nebraska, Minnesota, Iowa, Missouri, Illinois, Kentucky, Michigan, Indiana, and Ohio). The model performed best in South Dakota in spite of underestimations observed in the western regions (Fig. 14c). This was because most corn planted fields were heavily concentrated in the eastern regions (Fig. 1b). Consequently, the negative error observed in the western regions had less impact on the state level grain yield in South Dakota. In the case of Nebraska, the state level corn yields were continuously underestimated after 2006 (Fig. 16). This bias error may be caused by expansion of irrigated corn fields in central and eastern Nebraska, where the yield estimation error was less than −1.0 t/ha in most counties (Fig. 14c). The 5 year average of irrigated corn area increased from 1,135,000 ha (2002–2006) to 1,267,000 ha (2007–2011) in this region (codes of Agricultural Statistics Districts: 10, 20, 50, 70, and 80). Considering the coarse spatial resolution of MODIS (250 m/pixel at nadir), the degradation of estimation accuracy caused by the mixed-pixel effect would be unavoidable, especially outside the Corn Belt, where corn fields are sparsely distributed. Even though the model could not estimate the absolute level of state level corn yield with enough accuracy for practical use, the MODIS-estimated yields were comparable in variation pattern to the NASS derived statistics in several states including Colorado, Texas, Kansas, Oklahoma, Louisiana, West Virginia, Virginia, South Carolina, New Jersey, and Florida. This result implies that there is still plenty of potential for bias correction to expand the applicable coverage of the MODIS-based yield estimation model.

7. Discussion and conclusion

This study developed a model for corn grain yield estimation based on MODIS WDRVI ($\alpha = 0.1$). The main feature of this model was the incorporation of a MODIS-based crop phenology detection method called the “Shape Model Fitting method (SMF).” The SMF method was able to reveal the detailed spatio-temporal distribution of corn silking stages all over the U.S. By comparing the results with statistical data from NASS-CPR on a state level, it was verified that the SMF method was able to detect the median dates of key phenological stages from time series MODIS WDRVI ($\alpha = 0.1$) observations with high accuracy. NASS-CPR was unable to explain county level crop phenology because of its coarse statistical unit (ASD or state level). That is to say, there were few sources of information providing the spatio-temporal pattern of crop phenology with high resolution. Therefore, the establishment of a crop phenology detection method represented a momentous step in the development of a satellite based crop yield estimation model. Thus, this study integrated the SMF method with the approach of yield estimation using WDRVI (Guindin-Garcia, 2010) to obtain a yield estimation model. It was found that the smoothed MODIS WDRVI ($\alpha = 0.1$), observed at 7–10 days before the MODIS derived silking stage, showed the best correlation with the final corn grain yield at multiple scales from field to county level. As a result of the spatial comparison in corn grain yield, it was also found that the MODIS derived estimates showed the same spatial pattern of high yield regions (more than 10 t/ha) as the USDA/NASS derived statistics from 2000 to 2011. However, the model tended to underestimate the corn grain yield in

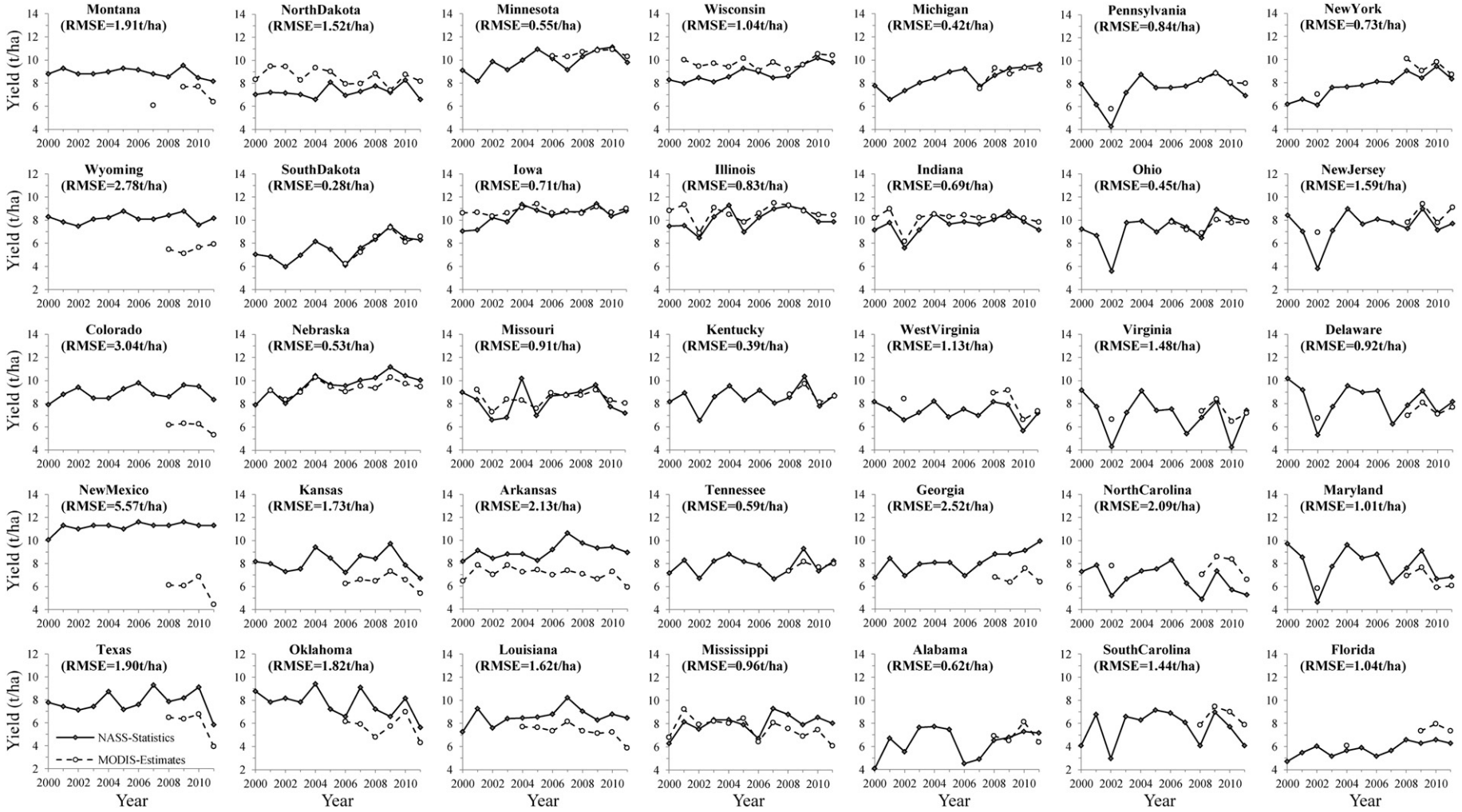

Fig. 16. MODIS-estimated and NASS-derived corn grain yield from 2000 to 2011 in 35 states.

three major irrigated regions, which were the Midwestern region fed by the Ogallala Aquifer, the downstream basin of the Mississippi, and the southwestern region of Georgia. In addition, the model also tended to overestimate the corn grain yield around the outlying regions of the U.S. Corn Belt, including the East Coast, North Dakota, Minnesota, Wisconsin, and Missouri. The MODIS-based corn yield estimation model was subject to, probably unavoidable, error caused by the mixed-pixel effect in half of the states studied. Moreover, there remain many other tasks to be solved in order to establish an early prediction model of corn grain yield that could predict final corn grain yield at the midterm crop growing period without relying on the release date of NASS-CDL. However, this study confirmed that the MODIS WDRVI ($\alpha = 0.1$) based model can predict the annual variation of state level corn grain yield with high accuracy in the major corn producing states (South Dakota, Iowa, Illinois, Indiana, Ohio Michigan, and Nebraska).

Acknowledgments

We offer special thanks to Mr. Dave Scoby for providing the field measurement data related to crop phenology and biophysical parameters. We are grateful to Dr. Tetsuhisa Miwa of NIAES for his valuable comments on statistical work. This study was conducted under memorandum of agreement between University of Nebraska-Lincoln and National Institute for Agro-Environmental Sciences, Japan.

References

Badhwar, G. D., Carnes, J. G., & Austin, W. W. (1982). Use of Landsat-derived temporal profiles for corn–soybean feature extraction and classification. *Remote Sensing of Environment*, *12*, 57–79.

Badhwar, G. D., & Henderson, K. E. (1981). Estimating development stages of corn from spectral data — An initial model. *Agronomy Journal*, *73*, 748–755.

Bauer, M. E. (1975). The role of remote sensing in determining the distribution and yield of crops. *Advances in Agronomy*, *27*, 271–304.

Boken, V. K., & Shaykewich, C. F. (2002). Improving an operational wheat yield model using phenological phase-based Normalized Difference Vegetation Index. *International Journal of Remote Sensing*, *23*, 4155–4168.

Bouman, B. A. M. (1995). Crop modeling and remote-sensing for yield prediction. *Netherlands Journal of Agricultural Science*, *43*, 143–161.

Chang, K. W., Shen, Y., & Lo, J. C. (2005). Predicting rice yield using canopy reflectance measured at booting stage. *Agronomy Journal*, *97*, 872–878.

Domenikiotis, C., Spiliotopoulos, M., Tsiros, E., & Dalezios, N. R. (2004). Early cotton yield assessment by the use of the NOAA/AVHRR derived Vegetation Condition Index (VCI) in Greece. *International Journal of Remote Sensing*, *25*, 2807–2819.

Doraiswamy, P. C., Sinclair, T. R., Hollinger, S., Akhmedov, B., Stern, A., & Prueger, J. (2005). Application of MODIS derived parameters for regional crop yield assessment. *Remote Sensing of Environment*, *97*, 192–202.

Ferencz, C., Bognar, P., Lichtenberger, J., Hamar, D., Tarscai, G., Timar, G., et al. (2004). Crop yield estimation by satellite remote sensing. *International Journal of Remote Sensing*, *25*, 4113–4149.

Gitelson, A. A. (2004). Wide dynamic range vegetation index for remote quantification of biophysical characteristics of vegetation. *Journal of Plant Physiology*, *161*, 165–173.

Gitelson, A. A., Wardlow, B. D., Keydan, G. P., & Leavitt, B. (2007). An evaluation of MODIS 250-m data for green LAI estimation in crops. *Geophysical Research Letters*, *34*, L20403.

Guindin-Garcia, N. (2010). *Estimating maize grain yield from crop biophysical parameters using remote sensing*. Doctoral thesis, Agronomy and Horticulture Department of University of Nebraska-Lincon Avaiable at: http://digitalcommons.unl.edu/agronhortdiss/21/(pp. 115).

Guindin-Garcia, N., Gitelson, A. A., Arkebauer, T. J., Shanahan, J., & Weiss, A. (2012). An evaluation of MODIS 8- and 16-day composite products for monitoring maize green leaf area index. *Agricultural and Forest Meteorology*, *161*, 15–25.

Hall, F. G., & Badhwar, G. D. (1987). Signature-extendable technology: Global space-based crop recognition. *IEEE Transactions on Geoscience and Remote Sensing*, 93–103.

Hatfield, J. L. (1983). Remote sensing estimators of potential and actual crop yield. *Remote Sensing of Environment*, *13*, 301–311.

Henderson, K. E., & Badhwar, G. D. (1984). An initial model for estimating soybean development stages from spectral data. *Remote Sensing of Environment*, *14*, 55–63.

Huete, A., Didan, K., Miura, T., Rodriguez, E. P., Gao, X., & Ferreira, L. G. (2002). Overview of the radiometric and biophysical performance of the MODIS vegetation indices. *Remote Sensing of Environment*, *83*, 195–213.

Idso, S. B., Hatfield, J. L., Jackson, R. D., & Reginato, R. J. (1979a). Grain yield prediction: Extending the stress–degree–day approach to accommodate climatic variability. *Remote Sensing of Environment*, *8*, 267–272.

Idso, S. B., Pinter, P. J., Hatfield, J. L., Jackson, R. D., & Reginato, R. J. (1979b). A remote sensing model for the prediction of wheat yields prior to harvest. *Journal of Theoretical Biology*, *77*, 217–228.

Idso, S. B., Reginato, R. J., & Jackson, R. D. (1977). Albedo measurement for remote sensing of crop yields. *Nature*, *266*, 625–628.

Kogan, F. N. (1997). Global drought watch from space. *Bulletin of the American Meteorological Society*, *78*, 621–636.

Labus, M. P., Nielsen, G. A., Lawrence, R. L., Engel, R., & Long, D. S. (2002). Wheat yield estimates using multi-temporal NDVI satellite imagery. *International Journal of Remote Sensing*, *23*, 4169–4180.

Liu, W. T., & Kogan, F. (2002). Monitoring Brazilian soybean production using NOAA/AVHRR based vegetation condition indices. *International Journal of Remote Sensing*, *23*, 1161–1179.

Maas, S. J. (1988). Using satellite data to improve model estimates of crop yield. *Agronomy Journal*, *80*, 655–662.

Moriondo, M., Maselli, F., & Bindi, M. (2007). A simple model of regional wheat yield based on NDVI data. *European Journal of Agronomy*, *26*, 266–274.

Nellis, M. D., Price, K. P., & Rundquist, D. (2009). Remote sensing of cropland agriculture. *The SAGE handbook of remote sensing* (pp. 368–380). SAGE Publications Limited.

Ozdogan, M., & Gutman, G. (2008). A new methodology to map irrigated areas using multi-temporal MODIS and ancillary data: An application example in the continental US. *Remote Sensing of Environment*, *112*, 3520–3537.

Ren, J., Chen, Z., Zhou, Q., & Tang, H. (2008). Regional yield estimation for winter wheat with MODIS-NDVI data in Shandong, China. *International Journal of Applied Earth Observation and Geoinformation*, *10*, 403–413.

Rudorff, B. F. T., & Batista, G. T. (1991). Wheat yield estimation at the farm level using TM Landsat and agrometeorological data. *Remote Sensing*, *12*, 2477–2484.

Sakamoto, T., Gitelson, A. A., Wardlow, B. D., Arkebauer, T. J., Verma, S. B., Suyker, A. E., et al. (2012). Application of day and night digital photographs for estimating maize biophysical characteristics. *Precision Agriculture*, *13*, 285–301.

Sakamoto, T., Wardlow, B. D., & Gitelson, A. A. (2011). Detecting spatiotemporal changes of corn developmental stages in the US Corn Belt using MODIS WDRVI data. *IEEE Transactions on Geoscience and Remote Sensing*, *49*, 1926–1936.

Sakamoto, T., Wardlow, B. D., Gitelson, A. A., Verma, S. B., Suyker, A. E., & Arkebauer, T. J. (2010). A Two-Step Filtering approach for detecting maize and soybean phenology with time-series MODIS data. *Remote Sensing of Environment*, *114*, 2146–2159.

Salazar, L., Kogan, F., & Roytman, L. (2007). Use of remote sensing data for estimation of winter wheat yield in the United States. *International Journal of Remote Sensing*, *28*, 3795–3811.

Serrano, L., Filella, I., & Penuelas, J. (2000). Remote sensing of biomass and yield of winter wheat under different nitrogen supplies. *Crop Science*, *40*, 723–731.

Tennakoon, S. B., Murty, V. V. N., & Eiumnoh, A. (1992). Estimation of cropped area and grain yield of rice using remote sensing data. *International Journal of Remote Sensing*, *13*, 427–439.

Unganai, L. S., & Kogan, F. N. (1998). Drought monitoring and corn yield estimation in Southern Africa from AVHRR data. *Remote Sensing of Environment*, *63*, 219–232.

USDA/FAS (2012). Grains: World markets and trade archives. Available at http://www.fas.usda.gov/grain_arc.asp last access date: Aug.6, 2012

Verma, S. B., Dobermann, A., Cassman, K. G., Walters, D. T., Knops, J. M., Arkebauer, T. J., et al. (2005). Annual carbon dioxide exchange in irrigated and rainfed maize-based agroecosystems. *Agricultural and Forest Meteorology*, *131*, 77–96.

Vermote, E. F., & Vermeulen, A. (1999). MODIS algorithm technical background document, atmospheric correction algorithm: Spectral reflectances (MOD09). *Nasa contract NAS5-96062*.

Wichelns, D. (2010). Agricultural water pricing: United States. *Background report supporting OECD study* (pp. 27) study. Available at: http://regulation2point0.org/wp-content/uploads/downloads/2010/03/Agricultural-Water-Pricing-United-States.pdf last access date: 7.Aug, 2012